

CHAPTER 4 RESULTS AND DISCUSSION

4.1 Chemical Composition of Rice Husk Ash by EDXRF

Table 4.1 showed the chemical composition of the rice husk ash by EDXRF. The main compositions were $\text{SiO}_2 \approx 87.20$ wt%, $\text{P}_2\text{O}_5 \approx 1.64$ wt%, $\text{K}_2\text{O} \approx 6.23$ wt%, $\text{CaO} \approx 3.12$ wt%, $\text{MnO} \approx 0.82$ wt% and $\text{Fe}_2\text{O}_3 \approx 0.97$ wt% respectively. It was seen that the major composition of rice husk ash is SiO_2 because the major constituents of rice husk are cellulose, lignin and ash. The chemical constituents are found to vary from sample to sample which may be due to the different geographical conditions, type of paddy, climatic variation, soil chemistry and fertilizers used in the paddy growth. The silicon atoms are concentrated in the protuberances and hairs on the outer and inner epidermis of the husk.

Table 4.1 Chemical compositions of rice husk ash sintered at 1100 °C.

Compound	wt%					
	SiO_2	P_2O_5	K_2O	CaO	MnO	Fe_2O_3
RHA	87.20	1.64	6.23	3.12	0.82	0.97

4.2 Density and Molar Volume

Chemical composition, density, molar volume and thickness of glasses (measure by vernier caliper) are shown in Table 4.2. The density and molar volume of the barium-borate-rice husk ash glasses system are shown with different BaO contents. The replacement of BaO at the expense of all B_2O_3 and RHA leads to an increase in density from 3.0953 to 3.6649 g/cm^3 , consistent with an increase in the molar volume from 32.41 to 36.26 cm^3/mol as the modifier content increases (with an inflection at BaO = 60 wt%). These may be due to constancy in the number of NBOs which indicates that BaO in this glass is acting partly as network modifier. The change in molar volumes depends on the rates of change of both density and molecular weight. However the increasing rate of molecular weight is greater than that of the density.

Table 4.2 Chemical compositions, thickness, density and molar volume of barium-borate-RHA glass system.

RHA glass Sample	wt%			Density (g/cm^3)	V_m (cm^3/mol)	Thickness (mm)
	(x)BaO	(80-x) B_2O_3	RHA			
1	45	35	20	3.0953±0.0053	32.41	3.067±0.029
2	50	30	20	3.1514±0.0036	33.47	3.133±0.014
3	55	25	20	3.2671±0.0080	34.04	3.238±0.014
4	60	20	20	3.4314±0.0020	34.28	3.308±0.063
5	65	15	20	3.5180±0.0057	35.47	3.167±0.014
6	70	10	20	3.6649±0.0054	36.26	3.275±0.000

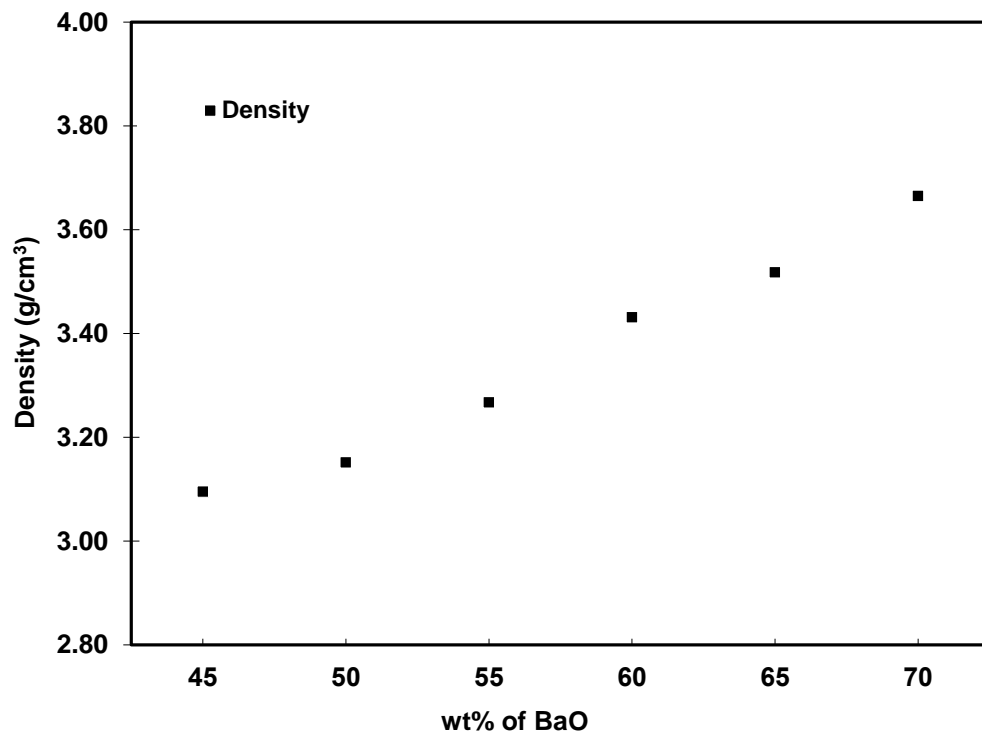


Figure 4.1 Dependence of the density of glass samples as a function of BaO content

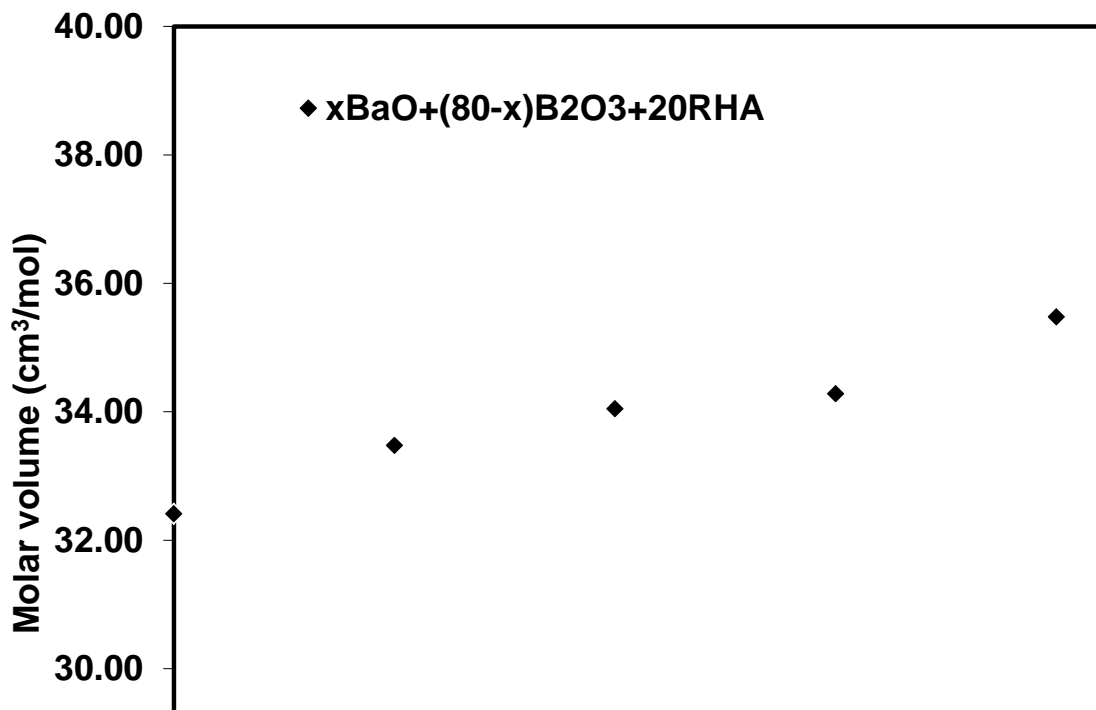


Figure 4.2 Dependence of the molar volume of glass samples as a function of BaO content

4.3 Refractive Index Measurement

Table 4.3 Chemical compositions, refractive index, molar refraction and molar electronic polarizability of barium-borate-RHA glass system.

RHA glass Sample	wt%			Refractive Index	R_m	α_m
	(x)BaO	(80-x)B ₂ O ₃	RHA			
1	45	35	20	1.5331±0.0010	10.06	3.99
2	50	30	20	1.5499±0.0006	10.66	4.23
3	55	25	20	1.5855±0.0011	11.41	4.53
4	60	20	20	1.6377±0.0029	12.31	4.88
5	65	15	20	1.6557±0.0003	13.03	5.17
6	70	10	20	1.6696±0.0005	13.54	5.37

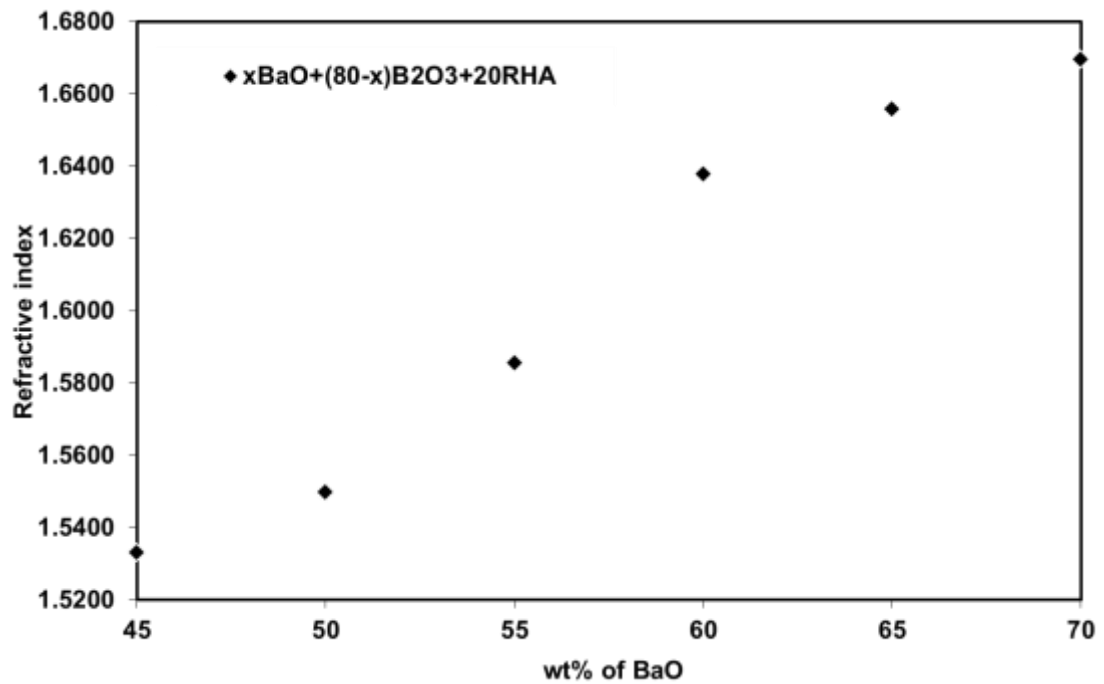


Figure 4.3 Refractive index of barium-borate-RHA glass system.

The refractive indices were measured by an Abbe refractometer, which permits the measurement of refractive indices up to 1.7 with an accuracy of 0.0002. A sodium lamp (D line = 589.3 nm) was used as the light source and mono-bromonaphthalene was used as the contact medium between the surface of the apparatus prism and the test sample. The refractive index of RHA glasses doped with BaO are from 1.5331 ± 0.0010 to 1.6696 ± 0.0005 . The molar refraction (R_m) of glass derived by Volf, Lorents and Lorenz is

$$R_m = \frac{(n_D^2 - 1)}{(n_D^2 + 2)} \left(\frac{m}{\rho} \right)$$

where n_D is the refractive index at 587.56 nm, ρ is the density and m is the molecular weight of the glass samples. The ratio (m/ρ) is the molar volume (V_m) and $R = (n_D^2 - 1)/(n_D^2 + 2)$ is known as the refraction loss. The molar refraction is related to the structure of the glass and it is proportional to the molar electronic polarizability of the material, (α_m), (in $\text{cm}^3 \times 10^{-24}$) through the following Clasius –Mosotti relation:

$$\alpha_m = \left(\frac{3}{4\pi N} \right) R_m$$

where N is the number of polarizable ions per mole and is assumed to be equal to the Avogadro's number N_A . The value $4\pi/3$ is known as Lorentz function. With α_m in (Å^3), can be transformed $R_m = 2.52 \alpha_m$.

4.4 UV-Visible Transmission Spectra

UV and visible transmission spectra were immediately measured for perfectly polished glass samples of equal thickness (3 mm). In order to investigate the optical properties of these glasses at various concentrations, the transmittance was measured as a function of wavelength in the range of 300-800 nm as shown in Fig. 4.4. All the glasses showed that the transmittance higher than 60% in the visible region.

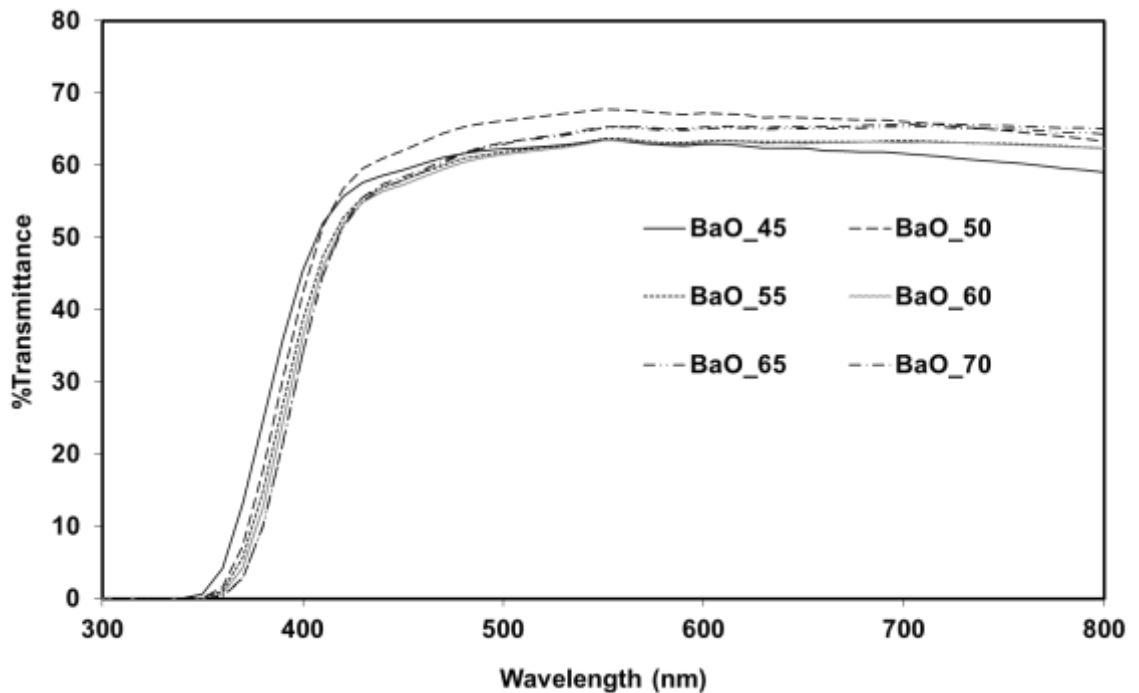


Figure 4.4 UV-VIS transmission spectra of barium-borate-RHA glass system.

4.5 Gamma-Ray Shielding Property

Figure 4.5 shows the typical 662 keV γ -ray spectra from ^{137}Cs as measured in our transmission experiment. The decrease of area in photopeak region with increasing of BaO content in glass showed ability for attenuation of γ -rays by glass sample. The mass attenuation coefficients of glass samples as shown in Table 4.3 were calculated from Eq. 2.34 and the theoretical values were calculated by WinXCom program [18, 19]. It has been found that the mass attenuation coefficients were increased with increasing of BaO content in glass matrix, indicating the better shielding properties. The experimental values of mass attenuation coefficient are in good agreement with the theoretical values as shown in Fig. 4.6. The statistical error in this experiment calculated from the standard error of 3 items (i) ray-sum measurement, which calculated from experiment, the ray-sum is product of linear attenuation coefficient (μ) with thickness (x), (ii) density measurement and (iii) thickness measurement.

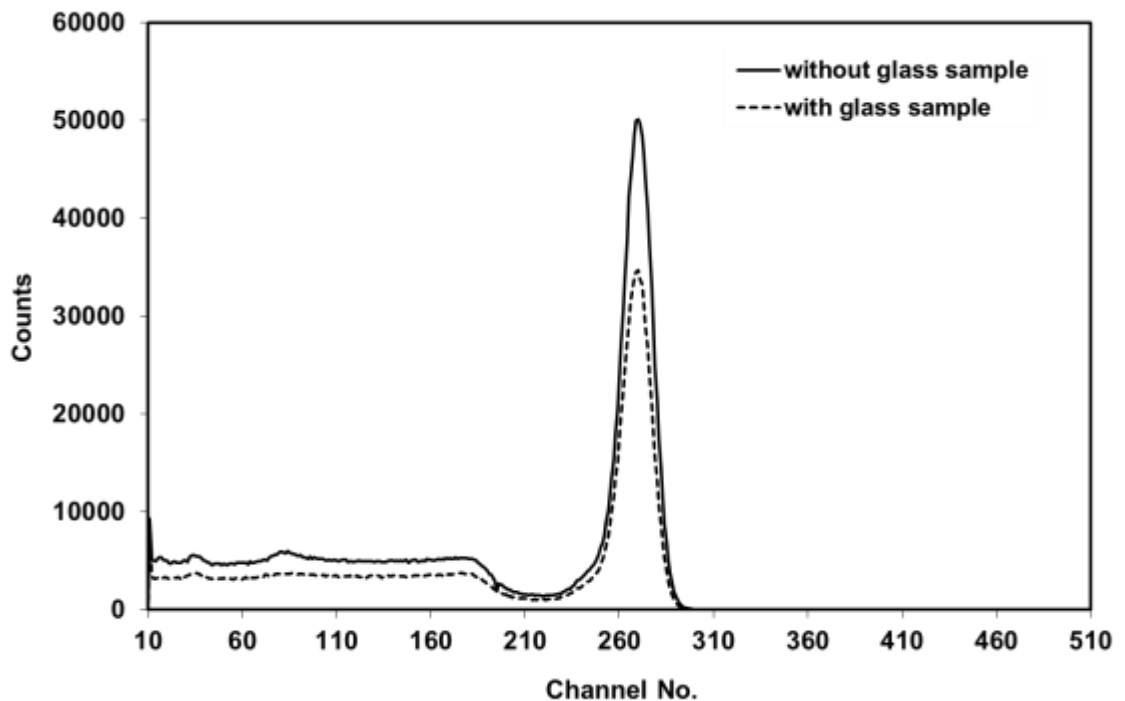


Figure 4.5 Typical 662 keV γ -rays spectra from a ^{137}Cs source measured with and without glass sample.

Table 4.4 Theoretical and experimental mass attenuation coefficients (cm^2/g) of barium-borate-RHA glass system at 662 keV γ -rays.

RHA glass Sample	wt%			μ_m (th) (cm^2/g)	μ_m (ex) (cm^2/g)	% RD
	(x)BaO	(80-x)B ₂ O ₃	RHA			
1	45	35	20	0.0767	0.0762±0.0010	0.65
2	50	30	20	0.0768	0.0765±0.0010	0.42
3	55	25	20	0.0769	0.0771±0.0008	0.29
4	60	20	20	0.0770	0.0769±0.0009	0.13
5	65	15	20	0.0771	0.0771±0.0009	0.03
6	70	10	20	0.0772	0.0770±0.0008	0.25

%RD= percentage relative difference between theory and experiment

Table 4.5 Theoretical and experimental of total atomic cross-section, total electronic cross-section and effective atomic number of barium-borate-RHA glass system at 662 keV γ -rays.

RHA glass Sample	$(\sigma_a)_{th}$ (b/atom)	$(\sigma_a)_{ex}$ (b/atom)	$(\sigma_e)_{th}$ (b/e)	Z_{eff} (th) (electrons/atom)	Z_{eff} (ex) (electrons/atom)
1	3.14	3.10	0.26	12.01	11.86
2	3.39	3.38	0.26	12.92	12.88
3	3.68	3.69	0.26	13.96	14.00
4	4.03	3.97	0.26	15.21	14.98
5	4.44	4.44	0.26	16.65	16.65
6	4.95	4.94	0.26	18.41	18.37

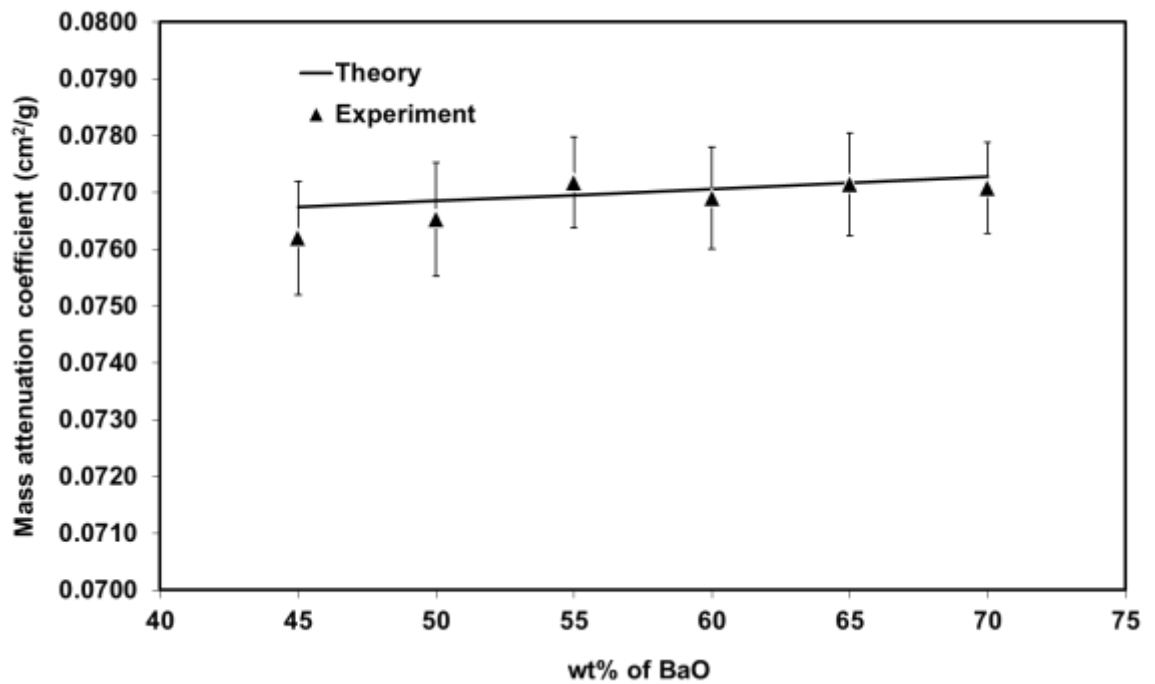


Figure 4.6 Variation of mass attenuation coefficient as a function of wt% of BaO at 662 keV γ -rays. The line is theoretical value and points are experimental values.

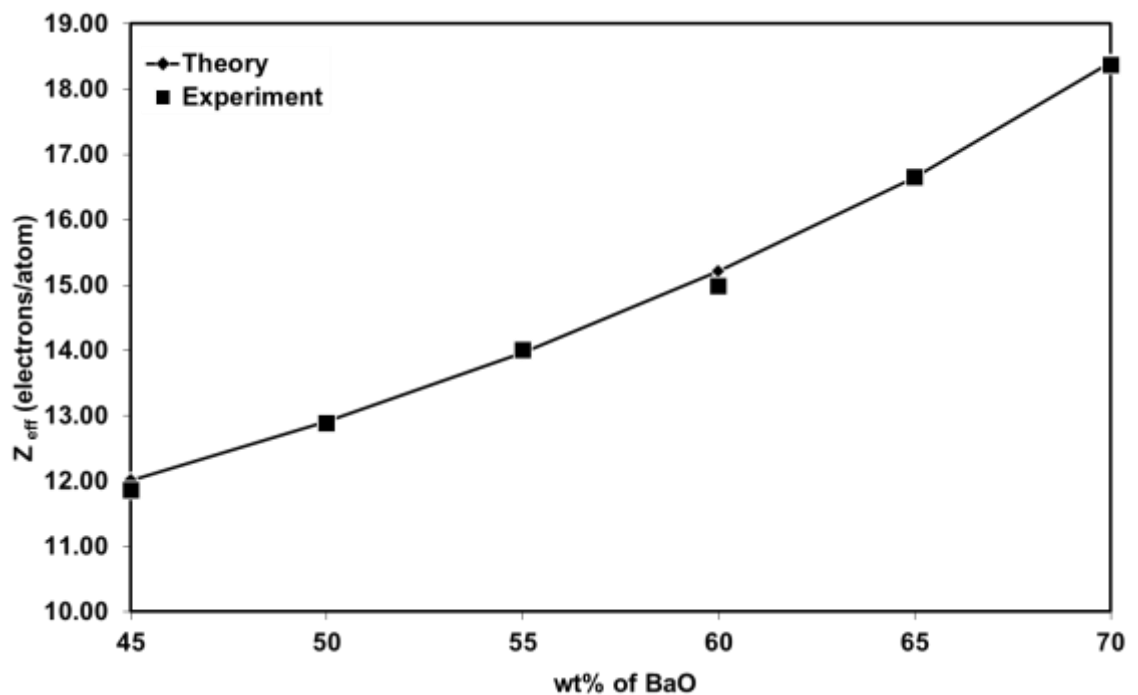


Figure 4.7 Effective atomic number at 662 keV γ -rays of barium-borate-RHA glass system. The line is theoretical value and points are experimental values.

The effective atomic number (Z_{eff}) have been determined using equation (2.42) are given in Table 4.5. Fig.4.7 shows good agreement between experimental and theoretical values of effective atomic number. It has been found that the effective atomic numbers were increased with BaO content. The relative different of mass attenuation coefficients were less than 1% reflecting the good detection system setup of transmission experiment. The value differences between experiment and theory suggested systematic errors; this may be due to non-stoichiometry ratio of glass formula after melting at high temperature.

The half value layers of glass samples as shown in Table 4.6 were evaluated from equation (2.38). Half value layers have been compared between glass samples and literature values of some standard shielding materials [1] as shown in Fig. 4.8. The better shielding properties of $x\text{BaO}:(80-x)\text{B}_2\text{O}_3:20\text{RHA}$ with increasing content of BaO can be observe with the decrease of the half value layers and the increase in density. At 70 wt% of BaO concentration, the radiation shielding has been found better than barite concrete. Ferrite concrete is also compared with glass samples and ferrite concrete show better shielding properties at this energy.

Table 4.6 The half value layers of barium-borate-RHA glass system at 662 keV γ -rays.

RHA glass Sample	μ_m (cm ² /g)	ρ (g/cm ³)	μ (cm ⁻¹)	HVL (cm)
1	0.0762	3.0953	0.23	2.93
2	0.0765	3.1514	0.24	2.87
3	0.0771	3.2671	0.25	2.75
4	0.0769	3.4314	0.26	2.62
5	0.0771	3.5180	0.27	2.55
6	0.0770	3.6649	0.28	2.45

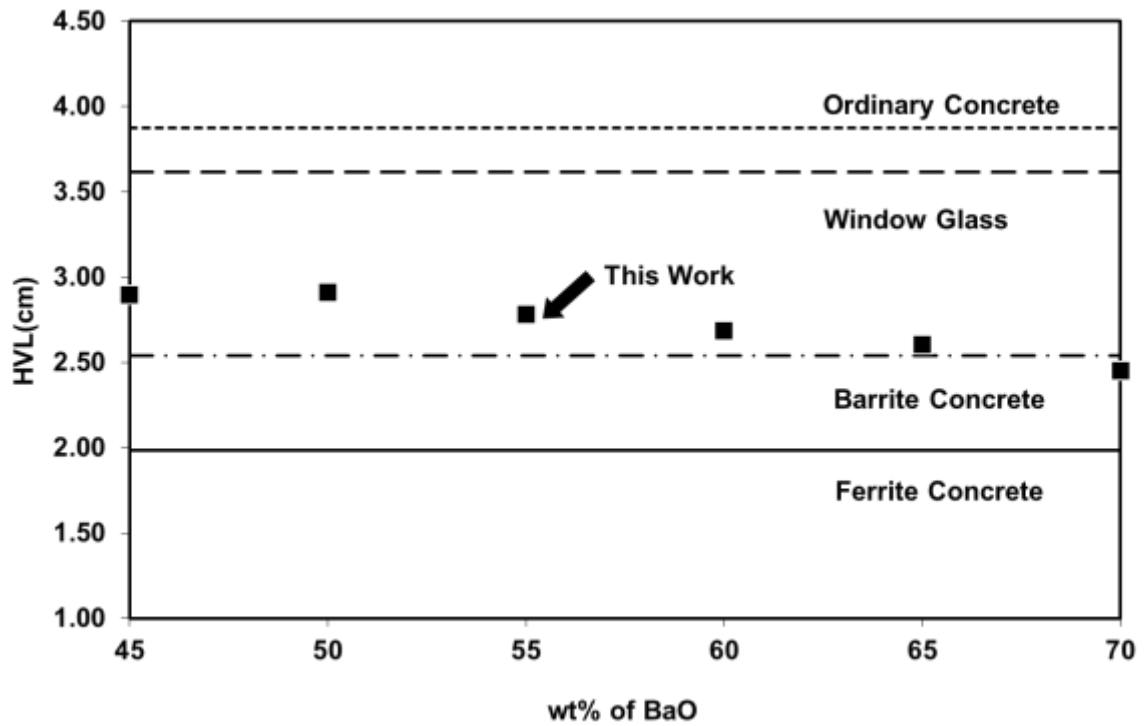


Figure 4.8 Variation of half value layer (HVL) as a function of BaO concentration at photon energy 662 keV compared with some conventional radiation shielding concretes and commercial window.